

# Modeling of hypervelocity impact on spacecraft honeycomb-core sandwich panels: investigation of projectile shape and honeycomb-core effects

Reihaneh Aslebagh<sup>1</sup>, [Aleksandr Cherniaev](#)<sup>1</sup>

<sup>1</sup> Department of Mechanical, Automotive and Materials Engineering, University of Windsor, 401 Sunset Ave., Windsor N9B 3P4, Canada

## 1 Introduction

In a typical satellite bus, most impact-sensitive equipment is situated in the enclosure of the structural sandwich panels, often – panels with a honeycomb core (*honeycomb-core sandwich panels*, HCSPs). As commonly used elements in satellite structures, these panels form the satellite's shape and are primarily designed to resist launching loads and provide attachment points for satellite subsystems [1]. With low additional weight penalties, their intrinsic ballistic performance can often be upgraded to the level required for orbital debris protection [2].

Previous studies investigated the effects of impact conditions (projectile speed and material) and HCSP design parameters (e.g., facesheet thickness and material) on their ballistic performance [3-8]. Other studies have focused on the development of numerical models with the aim of establishing best practices for simulations of hypervelocity impact (HVI) on HCSPs [9], or evaluating the effect of certain design parameters, such as the honeycomb cell size [10 – 12]. A common feature of all of these studies is that they considered only one shape for the impactor, i.e., a spherical projectile.

At the same time, it has been recognized and confirmed by multiple studies involving other shielding systems that non-spherical impactors can be significantly more destructive. In particular, disk-shaped impactors were noted as being among the most dangerous projectile shapes [13 - 15], especially those impacts when the disk axis is orthogonal to the projectile velocity vector (“high-pitch” disk penetrators) [16].

To address a lack of research into the effects of projectile shape in HVI on HCSPs, authors of the present study developed a detailed and verified numerical model of a HCSP in LS-DYNA and used it to investigate the effect of high-pitch-angle, disk-like projectile impacts on the protective properties of spacecraft sandwich structures with honeycomb cores. In addition to a “regular” disk shape, the impact scenarios considered here involved disk projectiles with a central hole (annulus-shaped impactors).

## 2 LS-DYNA model of HCSP

A combination of `*EOS_GRUNEISEN (*EOS_004)` and `*MAT_JOHNSON_COOK (*MAT_015)` was used to represent the behavior of the projectile (Al2017-T4) and facesheet (Al6061-T6) materials. Parameters of the material cards used for these alloys are provided in Ref. [17]. Behavior of the Al5052 core was represented by `*MAT_PLASTIC_KINEMATIC (*MAT_003)` with the yield strength and tangential modulus set to 193 and 0 MPa, respectively.

The impact conditions considered in this study involved normal angle collisions between a panel and a projectile, which are known to be the most conservative design scenarios for HCSPs due to the so-called *channeling effect of a honeycomb core*, in which honeycomb cells constrain the expansion of the cloud of high-speed projectile fragments, focusing the impact energy and momentum of the fragments onto a small area of the rear facesheet.

Our hypervelocity impact simulation model of a honeycomb-core sandwich panel developed in LS-DYNA simulation software is shown in Figure 1. The panel is represented by 1.3 mm-thick facesheets and a 50.8 mm-thick core. The in-plane size of the modeled piece was 70 x 70 mm. In the impact region, discretization of all parts involved 0.1 mm elements or SPH particles, a size that is consistent with the findings of an earlier study by Legaud et al. [9]. The particular setup illustrated in Fig. 1 (with a spherical 2.5 mm projectile) replicates the conditions of the NASA experiment described in [18] and denoted as HITF 9005, which was used in this study to verify the developed numerical model. A detailed description of the different parts of the model, and the methods used to represent these parts, is provided below.

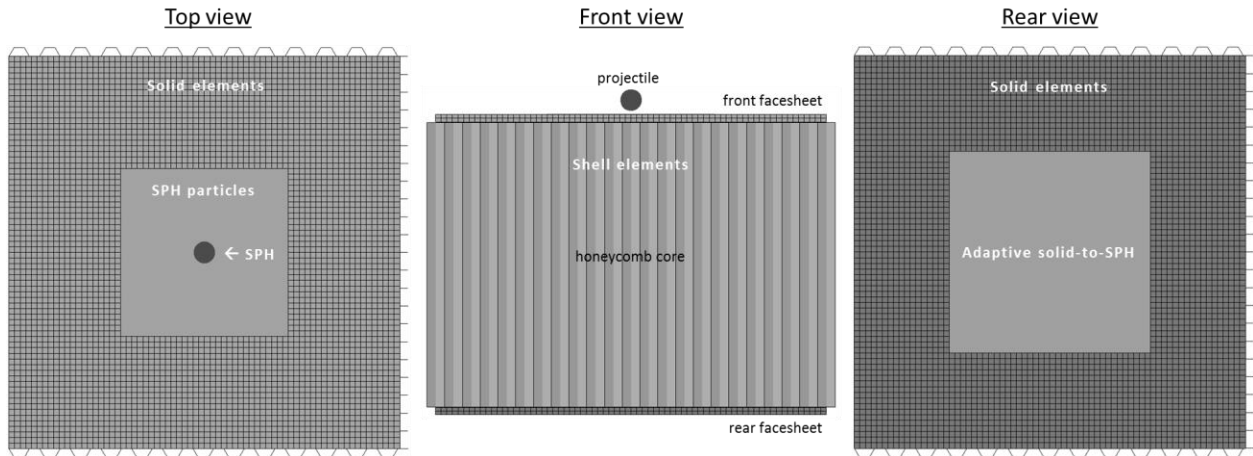


Fig. 1: General view of the simulation model

**Projectile.** Since a projectile, as a result of a hypervelocity collision with a sandwich panel, was expected to undergo complete disintegration and fragmentation, and to be subjected to extremely high deformations, a meshless method – smoothed particles hydrodynamics (SPH) – was employed to represent this part of the simulation model. Although projectiles with different geometries were modeled in this study, a common particle size of 0.1 mm was used for the discretization of each projectile type. A Eulerian SPH formulation #0, which was found in [9] to provide the highest accuracy in HVI simulations, was applied in all cases in this study. It was used with the quadratic spline kernel function, which was designed to relieve the compressive instability of SPH in HVI problems.

**Front facesheet.** The modeling of the front facesheet used both finite elements and SPH particles, as shown in Fig. 3. In particular, a 30 x 30 mm central region, where large deformations can be caused by the impact of the projectile, was fine-meshed using 0.1 mm SPH particles, while the rest of the front facesheet was discretized using 1.0 x 1.0 x 0.65 mm solid elements (two elements through-the-thickness of the facesheet). This roughly meshed region around the SPH part was used to prevent the reflection of stress waves from the boundaries of the SPH region. The interaction of the two parts (solid and SPH) was modeled using the `*CONTACT_AUTOMATIC_NODES_TO_SURFACE` algorithm in LS-DYNA. The interaction between the front wall and the projectile SPH particles was implemented using standard SPH interpolation.

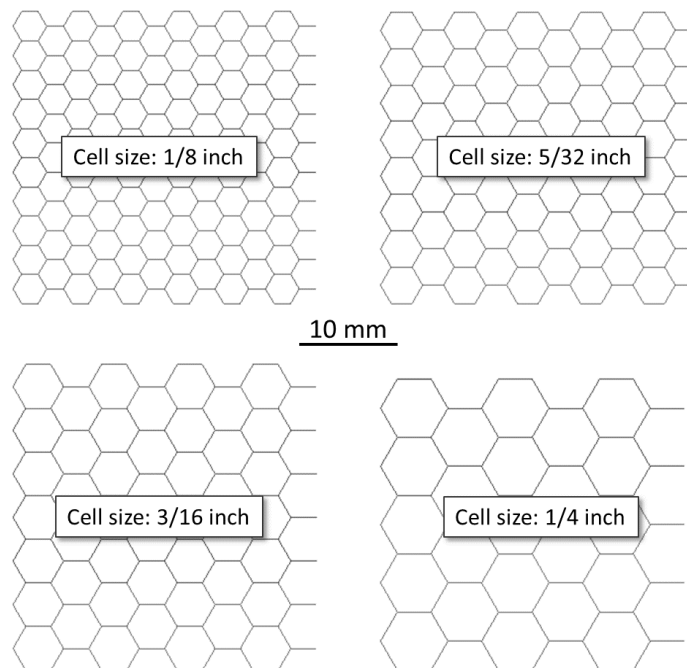


Fig. 2: The different sizes of honeycomb cell used in this study

*Honeycomb core.* The honeycomb cores of the sandwich panels were represented explicitly in the simulations, using fully integrated shell elements (formulation #16 in LS-DYNA with Reissner-Mindlin kinematics), as illustrated in Fig. 2. This explicit representation was employed in order to facilitate the modeling of the channeling effect of the honeycomb core on the cloud of hypervelocity fragments. The dimensions of the honeycomb cells corresponded to the HexWeb CR III grade of honeycomb from Hexcel with a nominal foil thickness of 0.0762 mm. The foil thickness was assigned to the parts of the honeycomb (single- and dual-wall) as an attribute of the corresponding shell element section. Although the original model replicating the conditions of the NASA HITF 9005 experiment involved a honeycomb with cells of size 1/8 inch, other cell dimensions were also used in subsequent simulations, and these are shown in Fig. 2. The contact between the SPH particles and the honeycomb core modeled with shell elements was implemented using the **\*CONTACT\_AUTOMATIC\_NODES\_TO\_SURFACE** algorithm in LS-DYNA.

*Rear facesheet.* It is well-known that although the SPH technique is often advantageous in modeling scenarios involving extreme deformation and fragmentation, the finite element method (FEM) in its Lagrangian implementation is well-suited to tracking the interfaces between materials. In order to exploit the advantages of both techniques simultaneously, a hybrid FEM/SPH approach was implemented for the facesheets using the LS-DYNA's **\*DEFINE\_ADAPTIVE\_SOLID\_TO\_SPH** keyword, which allowed for the local and adaptive transformation of Lagrangian solid elements (formulation #1) to SPH particles when the solid elements became highly distorted and inefficient. This conversion was triggered by the erosion of solid elements, which happened when the effective plastic strain in the element reached a level of 30%. The SPH particles replacing the eroded solid elements inherited all the nodal and integration point quantities of the original solids and were initially attached to the neighboring solid elements. This approach makes it possible to accurately capture different levels of damage to the rear wall, from small deformations (using solid elements) to very large ones, and, if necessary, to convert distorted solid elements to SPH particles. The interaction between the projectile and front facesheet fragments modeled with SPH and the solid elements of the rear facesheet was simulated using an eroding node-to-surface contact via the **\*CONTACT\_ERODING\_NODES\_TO\_SURFACE\_MPP** algorithm in LS-DYNA.

All of the hypervelocity impact simulations were conducted using the massively parallel processing (MPP) solver in LS-DYNA on a computer with twelve Intel Core i7-8700 CPUs and 32 GB of RAM. With these computational resources, the average runtime was around 40 h for simulations of 40  $\mu$ s after impact initiation.

### 3 Results and discussion

#### 3.1 Validation of the numerical model

Validation of the developed simulation model was achieved through a comparison of its predictions with the results of a physical experiment (HITF 9005) conducted by NASA and reported in [18]. In this test, a 2.5 mm Al2017-T4 spherical projectile with a speed of 6.91 km/s impacted on a honeycomb panel with 1.3 mm-thick Al6061-T6 facesheets, separated by a 50.8 mm-thick 1/8-5052-0.003 honeycomb core. A comparison between the simulation results and the physical HVI experiment conducted by NASA is shown in Figs. 3 and 4, for the damage to the front facesheet and the rear facesheet, respectively. It can be seen that a sphere of above-critical diameter traveling at 6.91 km/s induced full perforation of the sandwich panel, creating a near-circular entrance hole in the front facesheet and an irregularly shaped exit hole in the rear facesheet. The specific validation metrics included the following parameters: a) the size (diameter) of the hole in the front facesheet; and b) the size (effective diameter) of the hole in the rear facesheet. A comparison of the numerical values for these validation metrics is given in Table 1. As can be seen from the table, the predictions of the developed simulation model agree very well with the experimental results.

Part	Data source	Hole diameter, mm	Error, %	Reference
Front facesheet	NASA Experiment HITF 9005	6.9 (7.0 x 6.8)	--	[18]
	UWindsor simulation	7.1	+2.9	UWindsor data
Rear facesheet	NASA Experiment HITF 9005	4.4* (4.7 x 4.2)	--	[18]
	UWindsor simulation	4.1* (4.0 x 4.2)	-6.8	UWindsor data

Table 1: Predictions of the developed simulation model compared with the experimental results

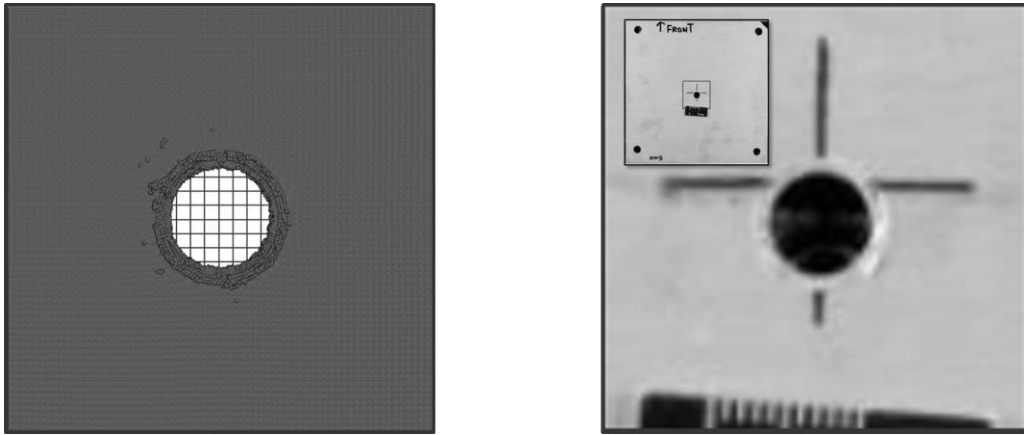


Fig.3: Front wall damage: simulation (grid cells: 1x1 mm) vs. NASA experiment (HITF 9005, [18])



Fig.4: Rear wall damage: simulation (grid cells: 1x1 mm) vs. NASA experiment (HITF 9005, [18])

### 3.2 Projectile shape effects

As discussed in the introduction section, disk-like penetrators with high pitch have been found to be among the most dangerous projectile shapes for single-purpose dual-wall (Whipple) shields. In this study, the verified HVI simulation model was used to extend this analysis to the case of impacts from high-pitch, disk-like projectiles on the honeycomb-core sandwich panels. In addition to computations with spherical projectiles, which were used as a reference, simulations were conducted using shapes such as simple disk-like impactors and projectiles in the form of a disk with a central hole, the latter of which are referred to here as “ring-shaped” impactors. The three projectile shapes considered in this study, along with their characteristic parameters, are shown in Fig. 5.

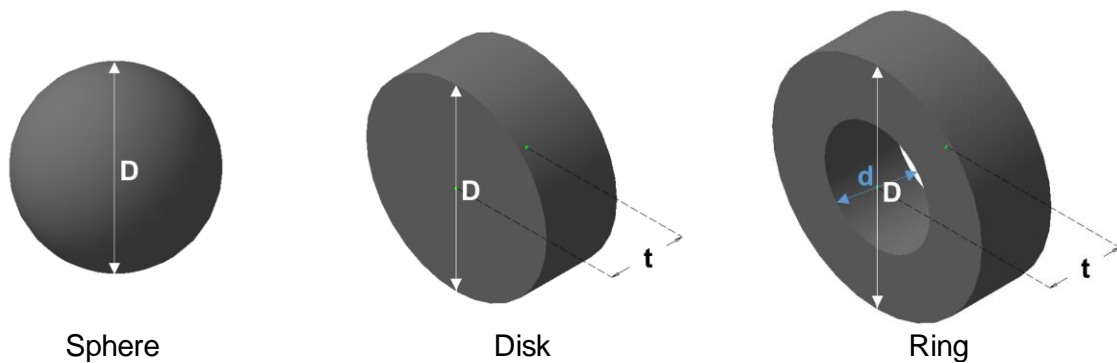


Fig.5: Sphere, disk and ring projectiles with equal volume

Spherical projectiles were characterized by the diameter ( $D$ ), disk projectiles by the diameter ( $D$ ) and thickness ( $t$ ), and ring projectiles by the thickness ( $t$ ), outer diameter ( $D$ ) and the ratio of the inner and the outer diameters ( $K$ ). The latter was kept constant at a value of 0.5 for all ring-shaped projectiles.

The investigation considered disk and ring impactors with different aspect ratios, defined as the ratio of the outer diameter to the thickness of the projectile,  $AR = D/t$ . The dimensions of all projectiles are listed in Table 2.

Type	Aspect ratio	D, mm	K = d/D	t, mm	V, mm <sup>3</sup>
Sphere	—	1.50	—	—	1.77
Sphere	—	1.20	—	—	0.90
Disk	1.50	1.20	—	0.80	0.90
Disk	3.00	1.51	—	0.50	0.90
Disk	4.50	1.73	—	0.38	0.90
Ring	1.50	1.32	0.5	0.88	0.90
Ring	3.00	1.66	0.5	0.55	0.90
Ring	4.50	1.90	0.5	0.42	0.90
Ring	3.00	1.53	0.5	0.51	0.70

Table 2: Parameters of the projectiles used in this study

The test matrix involved 12 numerical experiments, including two with spherical projectiles of sub-critical (1.2 mm) and above-critical (1.5 mm) diameter. These were used to verify the model and to establish the ballistic limit of the sandwich panel. The specific objectives of the calculations were as follows:

1. To understand the perforating ability of disk and ring-shaped projectiles, as compared to spherical impactors of the same mass;
2. To evaluate the effect of the aspect ratio on the perforating ability of disk and ring-shaped projectiles;
3. To investigate the effects of the projectile-honeycomb cell alignment and the size of the honeycomb cell on the ballistic performance of the honeycomb core sandwich panels, when hit with non-spherical projectiles.

To achieve the first and second goals, simulations were conducted with disk and ring projectiles with different aspect ratios of between 1.5 and 4.5. These projectiles had the same volume (and mass) as the sub-critical spherical projectile with  $D = 1.2$  mm that was shown not to perforate the HCSP with the 1/8 inch-cell honeycomb core. For the third goal, HV1 simulations were conducted for panels with different honeycomb cores (see Fig. 2) and different alignments between the projectiles and the honeycomb cells. This included projectiles that were roughly centered at the cell center and those aligned with a wall of the honeycomb before impact, as illustrated in Fig. 6. The corresponding virtual test matrix is provided in Table 3, and in addition to the projectile and honeycomb parameters, includes information about the alignment between the projectile and the honeycomb cell, and the outcome of each test. The latter is defined via a binary pass/fail output, where “fail” corresponds to full perforation of the panel’s rear facesheet. The termination time for all simulations was set to 40  $\mu$ s.

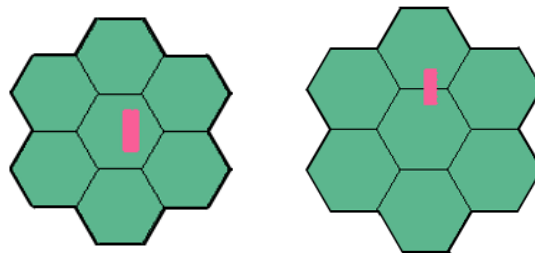


Fig.6: Alignment between the projectile and the honeycomb cell: cell-centered (left) and wall-centered (right) projectile

Simulation #	Projectile	Volume, mm <sup>3</sup>	Aspect ratio	HC cell size, inch	Projectile-cell alignment	Outcome
1	Sphere	1.77	—	1/8	center	Fail
2	Sphere	0.90	—	1/8	center	Pass
3	Disk	0.90	1.50	1/8	center	Pass
4	Disk	0.90	3.00	1/8	center	Pass
5	Disk	0.90	4.50	1/8	center	Pass
6	Ring	0.90	1.50	1/8	center	Fail

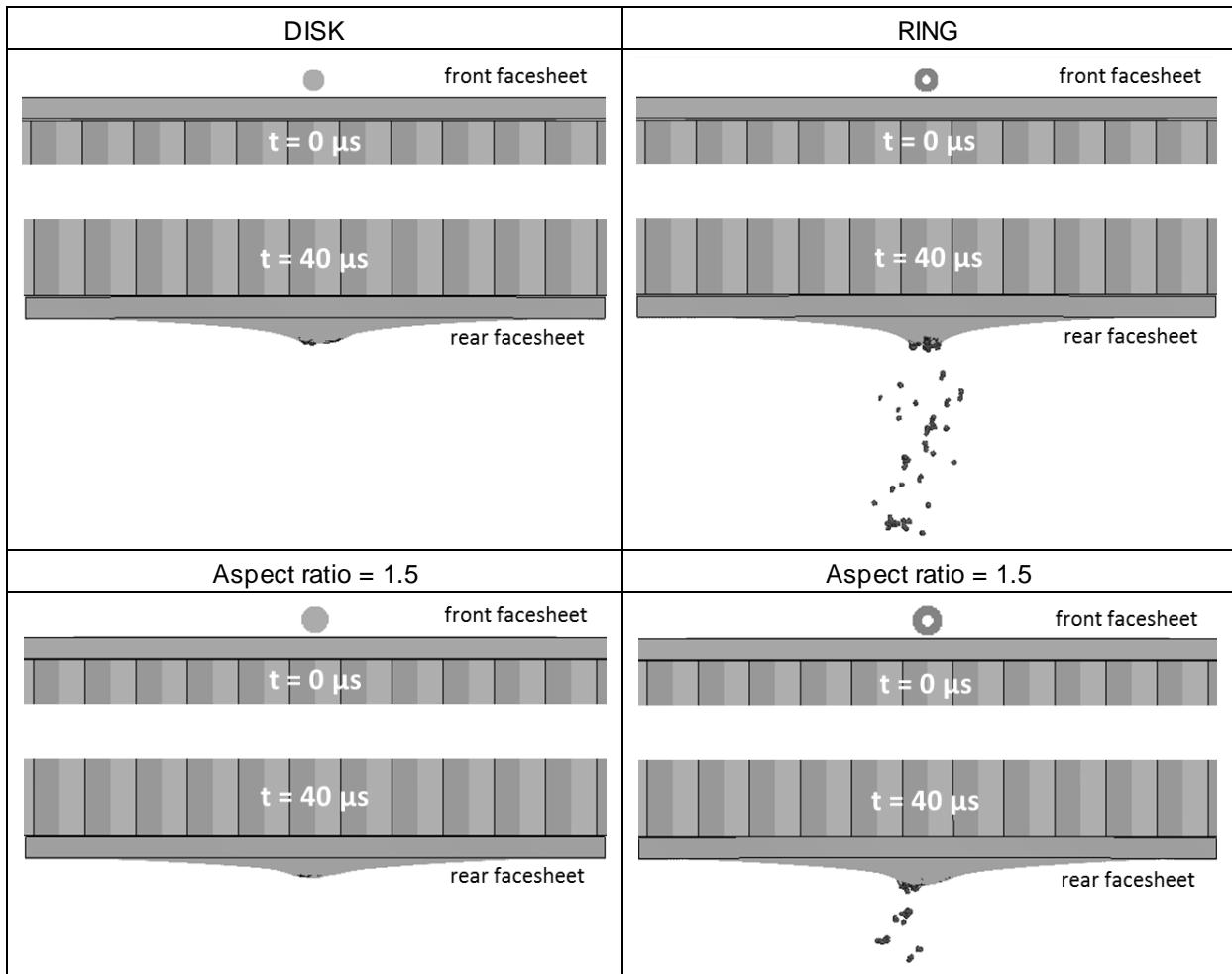
7	Ring	0.90	3.00	1/8	center	Fail
8	Ring	0.90	4.50	1/8	center	Fail
9	Ring	0.90	3.00	5/32	wall	Pass
10	Ring	0.90	3.00	3/16	center	Pass
11	Ring	0.90	3.00	1/4	wall	Pass
12	Ring	0.70	3.00	1/8	center	Pass

Table 3: Test matrix and outcomes of the numerical experiments

Figure 7 shows the setup and the results for simulations 3–8 (as shown in Table 3). As can be seen from the figure, all simulations with disk impactors gave the same results as the simulation conducted with the 1.2 mm spherical projectile of equal volume (and mass): no perforation of the rear facesheet was detected. Changing the aspect ratio of the disk projectiles within the range 1.5–4.5 did not have a noticeable effect on their penetrating ability. The opposite was true for the ring-shaped impactors: all three HVI simulations conducted with the ring projectiles under identical impact conditions resulted in perforation of the honeycomb-core panel, as illustrated in Fig. 7. These results reveal for the first time that ring-shaped impactors may be of higher concern than simple disk projectiles. This may be a consequence of the higher elongation of ring projectiles (for the same volume,  $D_{ring} > D_{disk}$ ), and of the complex interaction between the shock waves and the internal free boundaries of the ring, which combine to give a lower degree of fragmentation of the ring impactor upon collision with the front facesheet compared to its disk-shaped counterpart. The effect of the aspect ratio, which was varied from 1.5 to 4.5 was moderate. The size of the exit hole in the rear facesheet (the effective diameter of an irregular-shaped hole measured on a 0.1 x 0.1 mm grid) was:

- 0.7 mm for a projectile with AR = 1.5;
- 0.4 mm for a projectile with AR = 3.0; and
- 0.7 mm for a projectile with AR = 4.5.

This nonlinear variation in the size of the hole suggests the presence of several competitive mechanisms that affect the penetrating ability of ring projectiles when the aspect ratio is changed.



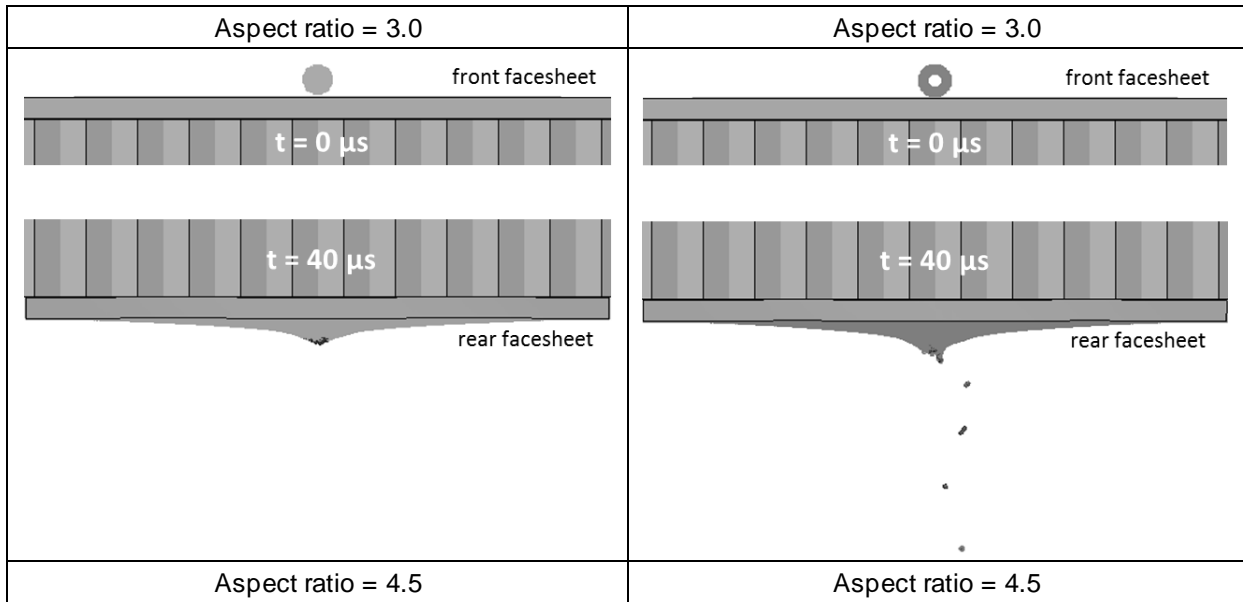
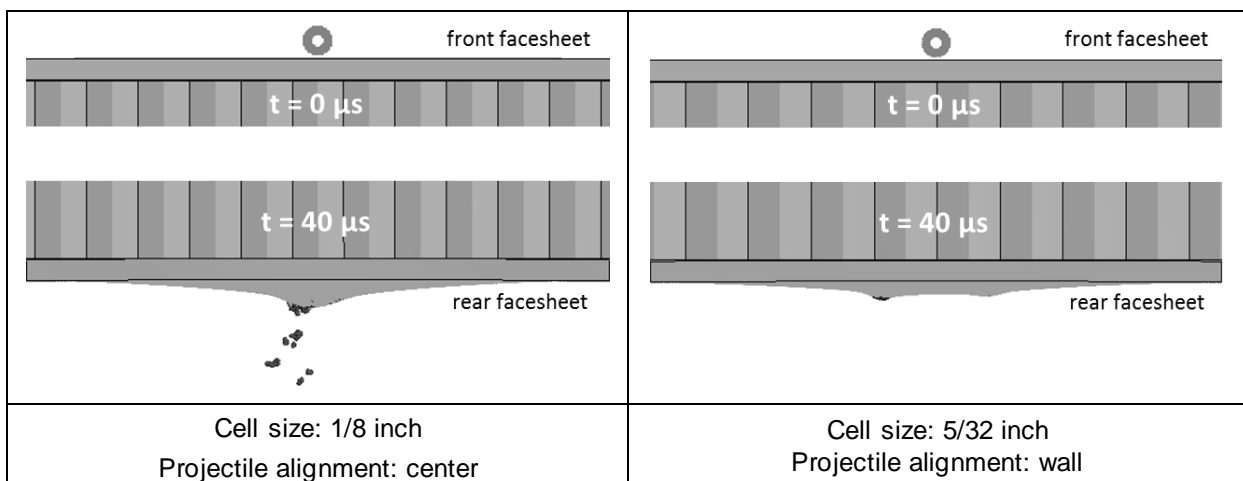


Fig.7: Effects of projectile shape and aspect ratio on damage to the rear facesheet (all projectiles have the same volume of 0.9 mm<sup>3</sup>)

The effects of the size of the honeycomb cell and the projectile/cell alignment on the ballistic limit of the HCSP was evaluated using a series of simulations with ring projectiles (AR = 3.0). In addition to 1/8 inch cells, these involved honeycomb cores with other cell dimensions of 5/32, 3/16 and 1/4 inch (simulations 7 and 9–11 in Table 3). The results of these analyses are shown in Fig. 8. As can be seen from this figure, both the cell size and the alignment can influence the outcome of the analysis. The effect of cell size can be seen from a comparison of the simulations that involved 1/8 and 3/16 inch honeycomb cores, with all other conditions being equal. As a result of an impact at 7 km/s, the panel with 1/8 inch cells was perforated, while the panel with 3/16 inch cells did not show perforation of the rear facesheet and was able to contain all of the fragments of the projectile and the front facesheet. This effect can be simply explained based on the additional space provided by larger honeycomb cells for expansion of the cloud of fragments, which means that the distribution of their momentum takes place over a larger area of the rear facesheet (less channeling), thus reducing the damage to it. Similar reasoning can be used to explain the influence of the alignment between projectile and honeycomb (“cell center” vs. “wall”) on the damage to the rear facesheet, as shown in Fig. 8. In case of a wall-centered impact, projectile fragments are channeled through two honeycomb cells, rather than only one in the case of cell centering. Notably, alignment with the wall not only reduces the severity of damage, but also changes its mode (giving two small, spaced bulges in the rear facesheet rather than one deeper bulge). This indicates that design calculations should consider the alignment of a projectile with the cell center as a more conservative scenario.



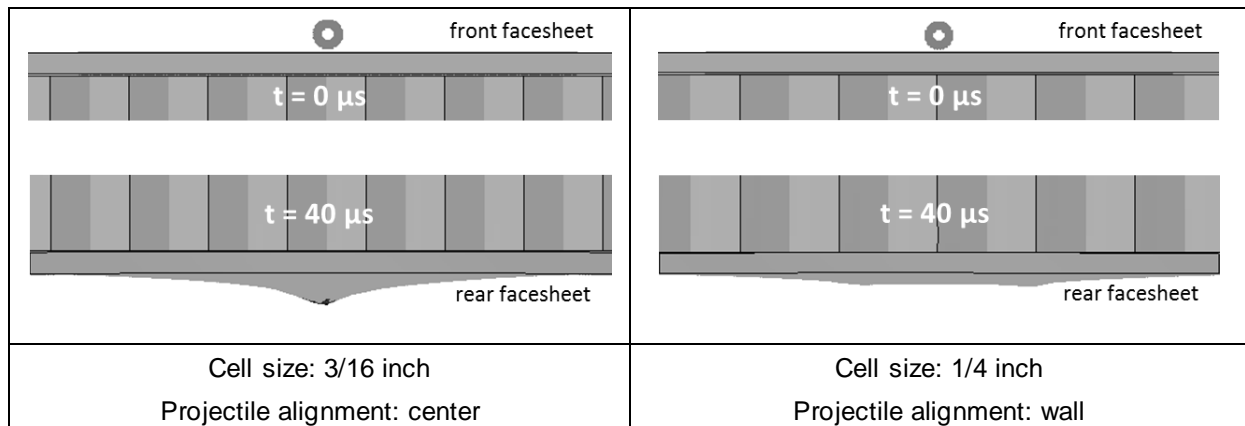


Fig.8: Effect of the size of the honeycomb cell on damage to the rear facesheet (all projectiles have the same aspect ratio of 3.0 and a volume of  $0.9 \text{ mm}^3$ )

#### 4 Summary

This study investigated the effects of projectile shape in hypervelocity impact on honeycomb-core sandwich structures. A model for the impact of a hypervelocity projectile on a sandwich panel with a 50.8 mm-thick aluminum honeycomb and 1.3 mm-thick aluminum facesheets was developed and verified against available experimental data. The model then was used to simulate collisions with disk and ring-shaped impactors traveling at 7 km/s. The following conclusions can be drawn from the results of these analyses:

- When hit by disk-shaped projectiles with an aspect ratio of between 1.5 and 4.5, no change in the ballistic limit of the panel was noted compared with impacts from spherical projectiles.
- Simulated collisions with ring-shaped projectiles demonstrated a significant reduction in the ballistic limit of the panel compared with impacts from disk-shaped and spherical projectiles, which is an important finding of this study. It was estimated that the volume of a ring-shaped impactor needed to perforate the sandwich panel was 1.65 times smaller than that of a spherical projectile. Currently available predictive models for sandwich panels do not account for projectile shape effects, and thus may result in non-conservative predictions of the ballistic limit.
- The aspect ratio of a ring projectile was varied from 1.5 to 4.5 and was shown to affect the size of the exit hole in the panel's rear facesheet: larger holes were predicted for smaller (1.5) and larger (4.5) aspect ratios, while a smaller perforation size was predicted for a medium aspect ratio (3.0), suggesting the presence of several competitive mechanisms that affect the penetrating ability of ring projectiles when their aspect ratio is changed.
- The cell size was found to significantly affect the ballistic limit of honeycomb panels subjected to an HVI at normal incidence. The increase in the ballistic limit (the outcome of the simulation changed from "perforation" to "no perforation") was achieved by the simple replacement of 1/8-inch cell honeycomb with a honeycomb with a cell size of 3/16 inch, all other conditions being equal. It should be noted that current BLEs do not account for the cell size effect in hypervelocity impacts with normal incidence, which identifies direction for their further improvement.
- The projectile/honeycomb cell alignment was found to affect the damage to the rear facesheet in the case of HVI at normal incidence. Based on the results of this study, we recommend aligning a projectile with the center of a honeycomb cell in simulations conducted for design purposes, in order to ensure that the most conservative scenario is explored.

#### 5 Acknowledgements

This work was financially supported by the Natural Sciences and Engineering Research Council of Canada through Discovery grant No. RGPIN-2019-03922. The authors would like to thank NASA and NASA Media Liaison Mr. Bert Ulrich for permission to reproduce experimental images (shown in Fig. 3 & 4) from NASA/TM-2015-218593 report.

#### 6 Literature

- [1] Bylander L. A., Carlström O. H., Christenson T. S. R., and Olsson F. G. A modular design concept for small satellites. In: *Smaller Satellites – Bigger Business?* 2002: 357–58.



- [2] Cherniaev A., Telichev I. Weight-efficiency of conventional shielding systems in protecting unmanned spacecraft from orbital debris. *Journal of Spacecraft and Rockets* 2016; 54(1): 75-89.
- [3] Taylor E.A., Herbert M.K., Vaughan B.A.M., and McDonnell J.A.M. Hypervelocity impact on carbon fibre reinforced plastic / aluminium honeycomb: comparison with Whipple bumper shields. *International Journal of Impact Engineering* 1999; 23 (1): 883–93.
- [4] Christiansen, E.L. 2009. Handbook for Designing MMOD Protection. NASA JSC-64399.
- [5] Ryan S., Christiansen E. 2010. Micrometeoroid and Orbital Debris (MMOD) Shield Ballistic Limit Analysis Program. NASA/TM–2009–214789.
- [6] Ryan, S., Schaefer, F., Destefanis, R., & Lambert, M. (2008). A ballistic limit equation for hypervelocity impacts on composite honeycomb sandwich panel satellite structures. *Advances in Space Research*, 41(7), 1152-1166.
- [7] Frost, C., & Rodriguez, P. (1997). AXAF hypervelocity impact test results. In *Second European conference on space debris*. Vol. 393, p. 423.
- [8] Schaefer, F. K., Schneider, E., & Lambert, M. (2004). Review of ballistic limit equations for composite structure walls of satellites. In *Environmental Testing for Space Programmes*. Vol. 558, pp. 431-444.
- [9] Legaud T., Le Garrec M., Van Dorsselaer N., Lapoujadet V. Improvement of satellites shielding under high velocity impact using advanced SPH method. 12th European LS-DYNA Conference, 2019, Koblenz, Germany.
- [10] Kang P., Youn S. K., and Lim J. H. Modification of the critical projectile diameter of honeycomb sandwich panel considering the channeling effect in hypervelocity impact. *Aerosp. Sci. Technol.*, vol. 29, no. 1, pp. 413–425, 2013.
- [11] Iliescu, L. E. Lakis, A. A. & Oulmane, A. Satellites/spacecraft materials and hypervelocity impact testing: numerical simulations. *Journal, M. Engineering, E. Centre, and D. Uk*, vol. 4, no. 1, pp. 24–64, 2017.
- [12] Schubert M., Perfetto S., Dafnis A., Mayer D., Atzrodt H., Schroder K. U. Multifunctional load carrying lightweight structures for space design. institute of structural mechanics and lightweight design, RWTH Aachen University , Fraunhofer Institute for Structural Durability and System Reliability LBF, Darmstadt , pp. 1–11, 2017.
- [13] Hu K., Schonberg W. P. Ballistic limit curves for cylindrical projectiles impacting dual-wall spacecraft systems. *Structures and Materials*, vol. 11. pp. 101–109, 2002.
- [14] Schonberg W. P., Williamsen J. E. RCS-based ballistic limit curves for non-spherical projectiles impacting dual-wall spacecraft systems. *International Journal of Impact Engineering*, vol 33, pp. 763–770, 2006.
- [15] Chhabildas L.C., Hertel E.S., Hill S.A. Hypervelocity Impact Tests and Simulations of Single Whipple Bumper Shield Concepts at 10 km/s. *Int. J. Impact Engng*, 1993; 14: 133-144.
- [16] Miller J. E. Considerations of oblique impacts of non-spherical, graphite-epoxy projectiles. *First Int'l. Orbital Debris Conf.* (2019).
- [17] Aslebagh R. Hypervelocity impact on satellite sandwich structures: development of a simulation model and investigation of projectile shape and honeycomb core effects. MASC thesis. University of Windsor (2021).
- [18] Ryan S., Christiansen E. Hypervelocity impact testing of aluminum foam core sandwich panels. NASA/TM–2015–218593.